Computer Assisted Mechanics and Engineering Sciences, 9: 223–237, 2002.

Computer modelling of cable reinforced membranes

Marek Stanuszek
Institute of Computer Modelling, Faculty of Applied Physics and Computer Modelling
Cracow University of Technology, ul. Warszawska 24, 31-155 Cracow, Poland

(Received June 8, 2000)

This paper is intended to summarise the actual work in the area of large deformations of tension systems. The previously conducted research [23, 24] adds significant contributions to the understanding of the response characteristics of pneumatics and suspended membranes with wrinkling allowed. Here the attention will be focused on the applications of the one-dimensional tensioned cable systems. Two- and three-dimensional tensile structures, will be forced to work with compressed members. Since cables can not transmit any compressive forces a verified numerical algorithm, based on the monitoring of the load displacement path is proposed. The special computer code NAFDEM (Nonlinear Analysis by Finite Difference and Element Methods) [13] was adapted to solve undertaken highly nonlinear problems. Calculated results were verified numerically and compared with the solutions obtained by the numerical integration technique.

1. Introduction

Not only have tensioned structures become accepted solutions a covering large interior-support-free facilities but also their use seems to be increasing. They have commonplace appearance and supply standard solutions, providing covering for unobstructed large areas, such as recreational and sport facilities, semi-permanent storages, exhibition pavilions, or market places. Not only civil engineering applications of such structures may be found, but they can model household items used daily (bags, clothes) and even certain organs of our body (veins, muscles or skin).

Membrane structures usually are made of very light flexible materials like rubber, cloth, or translucent plastic sheets reinforced with cords, steel or plastic cables. Their shape can be maintained only due to a small internal overpressure (pneumatic structures) or an initial prestressing (suspension membranes or cable nets). It is assumed that the membrane and cables may carry only tension and work in a plane or uniaxial stress state. They cannot withstand compression or bending; if this happens, wrinkling zones in the membrane and cable slack may appear.

Traditionally in case of fabric roofs the main emphasis has been laid on the fabric or membrane component, with little attention paid to the cable components present in the majority of the tensioned structures. Edge cables are commonly used to gather the tensile forces from the membrane and redirect these distributed surface forces to conveniently located and isolated anchorage points at mast tops or foundation levels. Ridge or valley cables are often used to control or reduce fabric stresses as well as to influence the amount of the clearance underneath a membrane structure.

The analyses of cable-reinforced membrane shells performed in the past have usually neglected the membrane contribution. The membrane has been regarded only as a medium transmitting the loads to the cables. This is true if cable stiffness is much higher than that of the membrane and the membrane size is small. But in practice these conditions are not satisfied and the modelling of tensioned structures should consider the co-operation of cables and membrane in the whole system. Therefore it is desirable to treat both with the same algorithm and take their co-operation and interaction into account. Although the use of flexible cable structures in engineering is very popular and well known in literature [19, 20] and engineering practice [12, 18], the numerical algorithms useful in considering such special local effects as cable slack and membrane wrinkling are still lacking.

Thus applications of cable-modelled systems as well as their interaction with the membrane in reinforced structures were considered in this study. The complexity of such an analysis practically excludes any analytical techniques and only numerical considerations may yield the intuitively correct solutions.

2. Object of the analysis

Let us focus our attention on the tensioned structure represented by a membrane reinforced with edge cables as shown in Fig. 1. The rectangular membrane made of elastic material, fixed at the corners, was loaded by the traction forces $\mathbf{q}_o$. The behaviour of such a system will be considered in view of cable and membrane interaction.

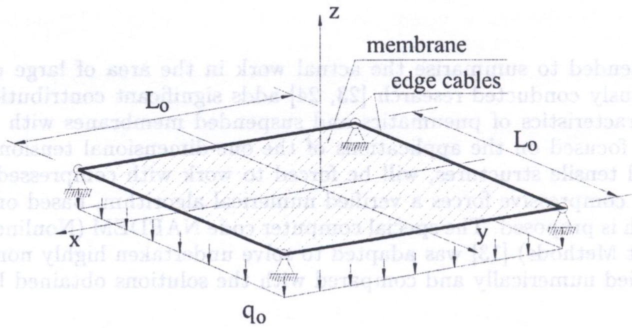

Fig. 1. Square membrane reinforced with edge cables

The special features distinguishing the cable and membrane tensioned structures from the more conventional structural forms (e.g. beams and shells) are:

- form of their surface strongly depends on the static and geometrical conditions;
- these structures are ideally flexible, carry only tension and work in a plane or uniaxial stress state. They cannot withstand compression or bending, in such a case folded zones in the membrane or cable slack will appear. These phenomena cause local instability of the structure and should be accounted for;
- the loading process of the separate cable element or membrane sheet is possible only if they are initially stressed in tension at least in one direction;
- after the load is applied, the structure usually undergoes large deflections caused by the initial internal flexibility.

As a result of the membrane and cable features listed above, acting loads trigger very large deformation of the structure. This deformation includes large displacements with possible membrane wrinkling and cable slack.

The static consideration of the cable systems in case of cable slack frequently deals with a mechanism. If the loads are transmitted through the membrane surface the deformation of the membrane with respect to the response of supporting or reinforcing cables has to be calculated. Hence the mathematical model of co-operation between membrane and cables has to be considered. At first a full joining of membrane and cables will be assumed. The cables will run along the membrane edges and will have the same element edge nodes. In this approximation the cable slip will be excluded and the nodes stiffness will be accumulated. For the connection to work [22] the membrane wrinkling and resulting cable slack will be allowed for.

Although such a problem has been theoretically considered by many researchers, still the quest for the formulation best suited for the numerical analysis of the deformations of cable-reinforced membranes with wrinkling has not been concluded. The problem at hand belongs to the non-trivial boundary value problems with unilateral constraints. In such a case it is impossible to find any analytical solution and only numerical modelling may yield reasonable results.

For the last thirty years there have been many publications dealing with the analysis of tensioned structures. It is obvious that complex analysis of such systems needs to distinguish at least two configurations, initial and actual and formulate the problem within the theory of nonlinear continuum mechanics. In such a case only a limited subclass of flexible structures (axially symmetrical shape and load) may be solved analytically. The practical solutions in any arbitrary case may be obtained only if numerical method such as Numerical Integration Technique (NIT [26]), Finite Difference Method(FDM [28]) or Finite Element Method (FEM) [1–3, 6, 24] is applied.

The actual "state of the art" in the domain of analysis of flexible membranes with wrinkling was presented in [22]. In the present paper attention is focused on the application of a *natural approach* [1] to the case of cable systems as well as their interaction with compatible membrane elements. The literature devoted to the shaping of cable systems is very numerous, but the analytical solutions are rare and limited to the simple shapes.

Application of FEM to the analysis of large deformations of cables was initiated by Argyris and Scharpf in [3] and Argyris, Angelopoulos and Bichat in [2]. In these papers the authors used the concept of geometric and elastic stiffness matrices in *form finding* analysis. The initial form of the system satisfying the equilibrium conditions for the initial stress state is searched for. The force density method was the other technique applied in such a case by Schek [21]. The idea of this method is based purely on mathematical calculation of the equilibrium without considering the elastic properties of the structure. This technique was extended to a more general assumed geometric stiffness method for membrane systems by Haber and Abel in [10, 11]. In proposed technique the designer has to assume both the prestress distribution as well as the geometric stiffness of the system, which is not a trivial task at the beginning of the deformation process. Moreover this technique is unsuitable in case of local instability caused by membrane wrinkling and cable slack.

It is very important to point out here that the design process of cable systems includes three main stages coupled together. As pointed above, the flexible system can exist only under an initial tensioned stress state, which determines the initial shape of the structure. Therefore it is crucial for further analysis to establish the initial configuration of the system. In the literature [10, 21] this stage is called form finding, shape finding or initial equilibrium problem. It is important to distinguish this stage, with an assumed initial stress state, from the large displacements of the structure caused by the application of the external loads.

Besides the already mentioned mathematically based methods, the dynamic relaxation introduced and applied to cable systems by Day [8] and Lewis et al. [16] was used. The extensions of this technique to a prestressed net and membrane were performed by Barnes [4, 5], Wakefield [29] and Ong et al. [18]. This technique seems to be an attractive approach since the shape finding as well as large displacements can be accounted for within the same numerical algorithm. The fictitious motion of the system is traced from the beginning of the loading to the final equilibrium state using D'Alembert's principle. The convergence and speed of the iterative process is governed by the fictitious masses assigned to the nodes, the damping coefficient, and the time step size during integration process. The dynamic relaxation seemed to be very popular engineering technique, but it did not find any application in the case of membrane wrinkling and cable slack. An engineering simplification to approximate the geometric nonlinearity using Taylor's expansion in the description of the deformed shape of the cable proposed by Kwan [15] and Kneen [12] is also worthy of notice.

Special attention was devoted in the literature to improving the convergence of the iterative process. To this end a second order of approximation of cable element geometry was introduced by Gambhir and Batchelor [9] and Argyris et al. [1]. The latter also presents a family of higher order isoparametric cable and membrane elements. Numerical applications and mutual comparison of higher order cable and membrane elements were presented by the author in [25] and [24] respectively. The approach enhancement, using the curvilinear shape of the initial cable geometry resultant of loads, was successfully considered by Pałkowski [20].

The early use of the finite element method with quadrilateral elements to analyse the nonlinear behaviour of cable-reinforced air-supported structures was considered by Li and Srivastava [17]. In this work the pattern of the cable net was assumed to be the same as for membrane elements, and any wrinkling or cables slacking at point of contact was neglected. The complete finite element approximation of both membrane and cables was presented consistently by Tabarrok and Qin in [27]. In the paper three main stages in the design process of tensioned structures were distinguished, i.e. form finding, load analysis and cutting pattern. The first one is based on determination of the initial shape of the structure satisfying the architectural and statical requirements while the second requires the investigation of the system response to the various service loads and the third is in the plane fabric layout stage determination. In [27] the cable and membrane co-operation as well as the convergence of the iterative algorithm in case of local instability were not considered. These will be undertaken in our study.

3. Large deformations of tensioned structures – finite element formulation

The tensile cable reinforced membranes are, in practice, shear-free prestressed mechanisms in which the form is governed by the surface and cable stress distribution.

As has been pointed out at the introduction, the large displacements and deformations as well as uniaxial boundary conditions are characteristic features of the considered structures and result in the geometrical nonlinearity of the problem. The essential feature of this nonlinearity is that equilibrium equations must be written with respect to the deformed geometry – which is not known in advance. Therefore the initial and actual system configurations, shown in Fig. 2, have to be distinguished, hence the *Total Lagrange* approach will be applied.

The complete formulation of membrane elements with wrinkling, applied in this paper, was presented by author the in [22]. Hence only certain modifications for cable elements allowed for slack will be presented. To preserve the membrane and cable compatibility, the main characteristics of the cable elements will be recalled based on [1, 25] and revised.

Two node isoparametric cable elements with linear approximation of the geometry and strain field will be considered. The geometry of the element during the deformation process is shown in Fig. 2, and will be described in the initial undeformed configuration by the geometry vector

$$ {}^{o}\mathbf{x} = {}^{o}\mathbf{x}(\xi_1\,,\xi_2), \qquad \text{where} \quad \xi_{1,2} \in \langle 0, 1\rangle \tag{1}$$

while in the actual configuration

$$ \mathbf{x} = {}^{o}\mathbf{x} + \mathbf{u} = \mathbf{x}(\xi_1\,,\xi_2). \tag{2}$$

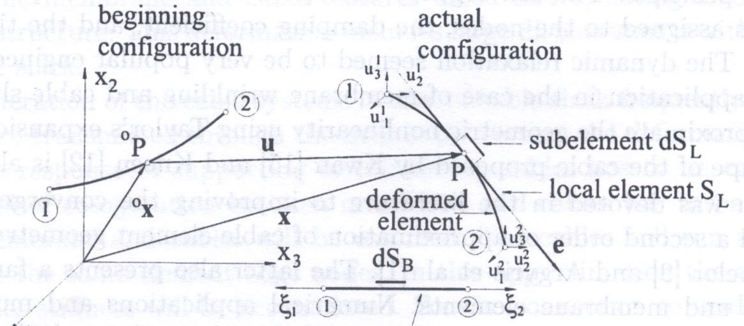

Fig. 2. Basic, initial and actual configurations of the cable element

In both configurations the so-called local element will be defined as a simple two node element tangent to the total element (Fig. 2) with length measures equal to

$$ {}^{o}m = ({}^{o}\mathbf{x}^{t}_{\|e}\,{}^{o}\mathbf{x}_{\|e})^{\frac{1}{2}}\,, \qquad m = (\mathbf{x}^{t}_{\|e}\mathbf{x}_{\|e})^{\frac{1}{2}} \tag{3} $$

in the initial and actual configurations respectively. The symbol $_{\|e}$ denotes the directional derivative in the direction of $\mathbf{e}$ vector and the superscript ^{o} denotes the reference to the undeformed configuration. The local element in the actual configuration can be mapped to the basic element in the reference configuration by the rule

$$ \mathbf{x}_L = x_{L1}\xi_1 + x_{L2}\xi_2\,, \qquad \xi_{1,2} \in \langle 0,1\rangle \tag{4} $$

where x_{L1} and x_{L2} are the local nodal co-ordinates of element S_L.

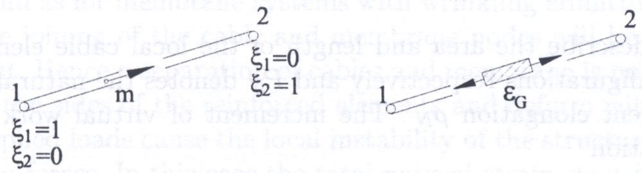

Fig. 3. Natural co-ordinates and strain of cable element

The description of the element deformation will be presented based on the *natural approach* which separates the real element deformation (change in length) from its rigid motion (rotation and shift). In this approximation the position of the current point of the element will be described by two dependent co-ordinates $\{\xi_1\,,\xi_2\}$ (Fig. 3), where $\xi_1+\xi_2=1$ (this preserves the compatibility of description of the geometry and the displacements for cable and membrane elements [1]). The natural element elongation and its increment are presented as

$$ \rho_N = m - {}^{o}m, \qquad \delta\rho_N = \delta m. \tag{5} $$

In order to take into account the higher-order terms of Cauchy geometric equations, the Green strain and its increment take the forms (Fig. 3)

$$ \varepsilon_G = \frac{1}{2}\,\frac{m^2 - {}^{o}m^2}{{}^{o}m^2}\,, \qquad \delta\varepsilon_G = \frac{m}{{}^{o}m^2}\,\delta m. \tag{6} $$

Consequently, adequately to the Green strain, the Piola–Kirchhoff stress will be introduced by the incremental constitutive equation

$$ \delta\sigma_P = E_P\,\delta\varepsilon_G \tag{7} $$

where E_P is the linear elasticity modulus. Using the interpolating scheme for isoparametric elements the geometry and displacement fields may be represented by the nodal values as

$$ \mathbf{x} = (\mathbf{I}_3\mathbf{N})\mathbf{x}_I\,, \qquad \mathbf{u} = (\mathbf{I}_3\mathbf{N})\mathbf{u}_I\,, \tag{8} $$

where $(\mathbf{I}_3\mathbf{N}) = (\mathbf{I}_3\otimes N_1\,,\mathbf{I}_3\otimes N_2\,,\ldots\,,\mathbf{I}_3\otimes N_j)$; $\mathbf{N}$ is a sequence of j shape functions ($j=$ number of nodes); $\mathbf{I}_3$ represents the identity matrix, $\mathbf{x}_I$ and $\mathbf{u}_I$ are the hypervectors of the geometry and the displacements of element nodes, and $\otimes$ denotes the Kronecker-product.

The increment of change in the length of the element in actual configuration can be calculated as

$$ \delta m = \delta(\mathbf{x}^{t}_{\|e}\mathbf{x}_{\|e})^{\frac{1}{2}} = \frac{1}{2(\mathbf{x}^{t}_{\|e}\mathbf{x}_{\|e})^{\frac{1}{2}}}\,2(\mathbf{x}^{t}_{\|e}\delta\mathbf{x}_{\|e}) = \frac{1}{m}\,\mathbf{x}^{t}_{\|e}\,\delta({}^{o}\mathbf{x}+\mathbf{u})_{\|e} = \frac{1}{m}\,\mathbf{x}^{t}_{\|e}\,\delta\mathbf{u}_{\|e} \tag{9} $$

and using the interpolation scheme (8)

$$\delta m = \frac{1}{m} ({}^o\mathbf{x}_I + \mathbf{u}_I)^t (\mathbf{I}_3\mathbf{N}_{\|e})^t (\mathbf{I}_3\mathbf{N}_{\|e}) \, \delta\mathbf{u}_I = \frac{1}{m} \mathbf{b}\delta\mathbf{u}_I \,, \tag{10}$$

noindent where $\mathbf{b}$ is the so-called geometry matrix. Using this equation the strain increment can be presented as the product

$$\delta\varepsilon_G = \frac{1}{{}^om^2} \mathbf{b}\delta\mathbf{u}_I \,. \tag{11}$$

Equilibrium equations of the element in the actual state will be derived using the virtual work principle for the local element in the form

$$\delta(W_L) = \int_{S_L} \delta(\mathrm{d}W_L) = \sigma_P \delta\varepsilon_G \, {}^oA \, {}^oS_L = P_N \delta\rho_N \,, \tag{12}$$

where ${}^oA$, ${}^oS_L$, A, S_L describe the area and length of the local cable element (see Fig. 2) in the reference and actual configurations respectively and P_N denotes the natural axial force corresponding to the natural element elongation ρ_N. The increment of virtual work in the total element is represented by the equation

$$\delta W = \frac{1}{S_B} \int_{S_B} \sigma_P \delta\varepsilon_G \, {}^oA {}^oS_L \, \mathrm{d}S_B = \frac{1}{S_B} \int_{S_B} P_N \delta\rho_N \, \mathrm{d}S_B \,. \tag{13}$$

Substitution of Eq. (5) and Eq. (9) yields the increment of virtual work in terms of nodal displacements and actual geometry

$$\delta W = \left(\frac{1}{S_B} \int_{S_B} P_N \mathbf{B} \, \mathrm{d}S_B \right) \delta\mathbf{u}_I = \mathbf{U}_I^t \, \delta\mathbf{u}_I \tag{14}$$

where $\mathbf{B} = \mathbf{b}\frac{1}{m}$, $\mathbf{U}_I$ represents the nodal forces corresponding to the nodal displacements $\mathbf{u}_I$. Since Eq. (14) is valid for all increments of the displacement vector, the set of nonlinear equilibrium equations in terms of the Piola–Kirchhoff stresses or natural forces is found to be

$$\frac{1}{S_B} \int_{S_B} \frac{1}{{}^om_2} \sigma_P \mathbf{b} \, {}^oA {}^oS_L \, \mathrm{d}S_B = \frac{1}{S_B} \int_{S_B} P_N \mathbf{B} \, \mathrm{d}S_B = \mathbf{U}_I \,. \tag{15}$$

Consideration of two close configurations in equilibrium and calculation of the increment of nodal forces provides

$$\begin{aligned} \delta\mathbf{U}_I = (\mathbf{U}_I + \delta\mathbf{U}_I) - \mathbf{U}_I &= \frac{1}{S_B} \int_{S_B} (\mathbf{B} + \delta\mathbf{B})^t \, (P_N + \delta P_N) \, \mathrm{d}S_B - \frac{1}{S_B} \int_{S_B} \mathbf{B}^t P_N \, \mathrm{d}S_B \\ &= \frac{1}{S_B} \int_{S_B} \delta\mathbf{B}^t P_N \, \mathrm{d}S_B + \frac{1}{S_B} \int_{S_B} \mathbf{B}^t \delta P_N \, \mathrm{d}S_B + \frac{1}{S_B} \int_{S_B} \delta\mathbf{B}^t \delta P_N \, \mathrm{d}S_B \,. \end{aligned} \tag{16}$$

This takes a well-known form

$$\delta\mathbf{U}_I = \mathbf{k}_G \delta\mathbf{u}_I + \mathbf{k}_E \delta\mathbf{u}_I + \delta\mathbf{J}_I \,, \tag{17}$$

where

$$\mathbf{k}_G \delta\mathbf{u}_I = \frac{1}{S_B} \int_{S_B} \delta\mathbf{B}^t P_N \, \mathrm{d}S_B = \left(\frac{1}{S_B} \int_{S_B} \frac{1}{{}^om} \sigma_P (\mathbf{I}_3\mathbf{N}_{\|e})^t (\mathbf{I}_3\mathbf{N}_{\|e}) \, {}^oA \, \mathrm{d}S_B \right) \delta\mathbf{u}_I \,, \tag{18}$$

$$\mathbf{k}_E \delta\mathbf{u}_I = \frac{1}{S_B} \int_{S_B} \mathbf{B}^t \delta P_N \, \mathrm{d}S_B = \left(\frac{1}{S_B} \int_{S_B} \frac{m^2}{{}^om^3} E_P \, {}^oA \, \mathbf{B}^t \mathbf{B} \, \mathrm{d}S_B \right) \delta\mathbf{u}_I \,, \tag{19}$$

$$\delta\mathbf{J}_I = \frac{1}{S_B} \int_{S_B} \delta\mathbf{B}^t \delta P_N \, \mathrm{d}S_B \tag{20}$$

are the elastic and geometric stiffness matrices respectively and $\delta \mathbf{J}_I$ denotes the error in the nodal load vector due to numerical calculations. Corresponding nodal forces in case of *dead* load represented by the intensity vector $\mathbf{q} = \{q_1, q_2, q_3\}$ may be calculated as the equivalent forces by the rule

$$\delta \mathbf{u}_I \mathbf{P}_I = \frac{1}{S_B} \int_{S_B} \delta \mathbf{u}^t \mathbf{q} S_L \, \mathrm{d}S_B \tag{21}$$

and using the interpolation scheme

$$\mathbf{P}_I = \frac{1}{S_B} \int_{S_B} (\mathbf{I}_3 \mathbf{N})^t \mathbf{q} S_L \, \mathrm{d}S_B \,. \tag{22}$$

The equations presented above let us consider the cable structures with slack cables using the same numerical algorithm as for membrane systems with wrinkling admitted [22]. For the simplicity of our consideration the joining of the cable and membrane nodes will be assumed, leading to the membrane reinforcement. Hence a separation of cables and membrane is not allowed. In the discrete model, cables lie along the sides of the reinforced elements and deform with them.

In some cases the applied loads cause the local instability of the structure. Certain cables slacken and do not transmit any forces. In this case the total natural strain start to be negative. This may be written in the natural measure as a sufficient codition of slack

$$\Rightarrow \quad \text{if } \varepsilon_G \leq 0 \text{ then } \sigma_{PN} = 0 \text{ and consequently } P_N = 0.$$

The switching off of certain cables in the cable model of the suspended structure is performed by incremental modification of the actual stress state of the cable which does not have any compressive rigidity. The main problem in the numerical analysis of large deformations of cable systems with slack cables admitted lies first in finding the right size of the load increment, to find the switching off of elements at the beginning of the slack state, and second, in the estimation of the fictitious rigidity at the nodes which are positioned at the intersection of slack cables, thus avoiding the singularity of the global stiffness matrix. It is obvious that the use of too large a load increment or of fictitious rigidity in switched-off nodes will drive an erroneous solution.

4. Numerical implementation

The Newton–Raphson technique was used to solve the set of nonlinear equilibrium equations (15) for cable-reinforced membrane structures. The flow chart of this technique is presented in Fig. 4. In this algorithm a verification step of the actual natural stress state in case of its negative value was introduced for cable as well as membrane elements. The algorithm was implemented in the computer system written in FORTRAN 90 called NAFDEM (*Nonlinear Analysis by the Finite Difference and Element Methods*) [13]. This system is based on the macro-language structure introduced by Zienkiewicz and Taylor [30]. The main advantage of this program is the joining of the finite element and difference methods in one tool, thus giving the possibility of their cooperation, not rivalry.

The system is built of five main units responsible for data control and memory management (PCONTR), data input (FEAP), mesh and geometry generation and modification (PMESH), modelling and control of the calculation process (MACR) and the post-processing (STOP). The structure of the system is presented in Fig. 5. After data preparation in the PMESH unit, the execution is transferred to PMACR segment, in which the required iteration scheme is performed. This scheme is executed in a sequence of macro-commands appropriate for the required algorithm. An important advantage of the NAFDEM lies in the monitoring of the iteration process. The system controls the successive displacement increments and loads residuum and any unexpected jumps are registered. Two norms applied by the system have to be satisfied in order to finish the iteration. The first one is the load residuum while the second represents the displacement increment value.

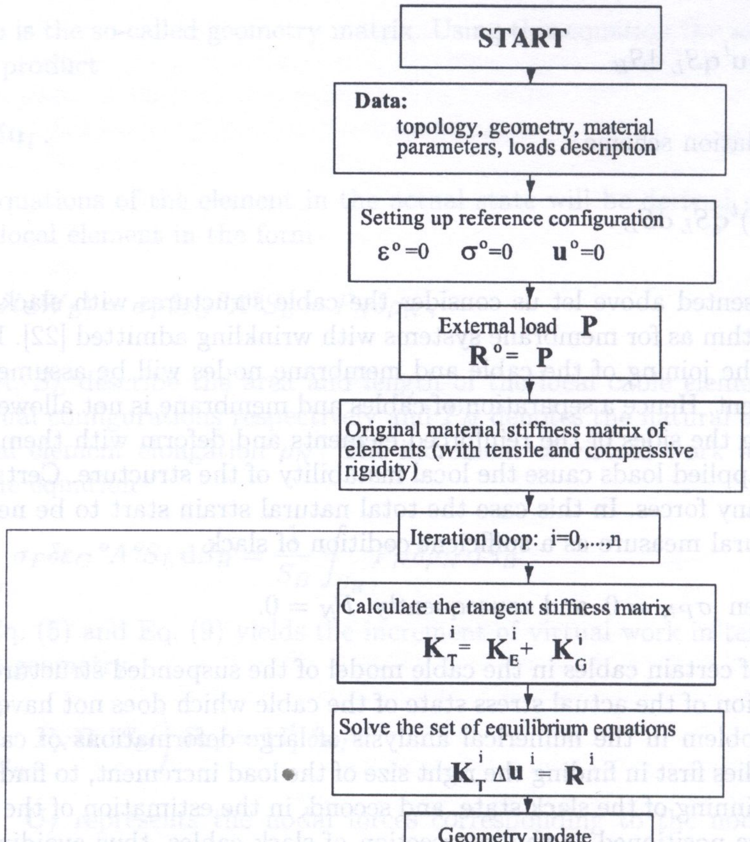

Fig. 4. Flow chart of nonlinear analysis of cable system

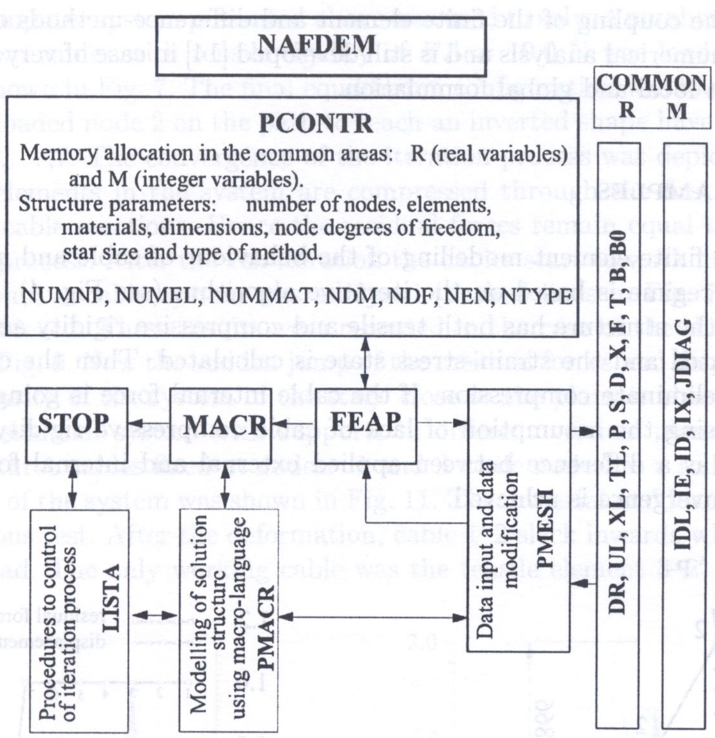

Fig. 5. Main segments in the NAFDEM system

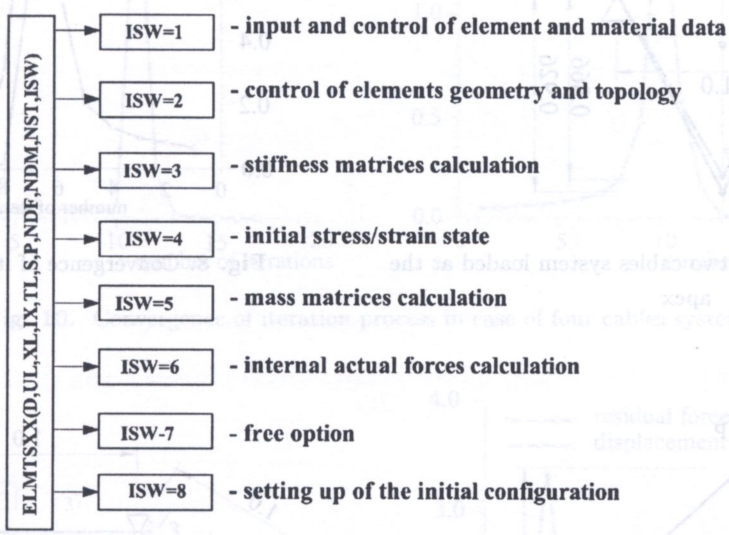

Fig. 6. The structure of the element subroutine

There is already a complex one-, two- and three-dimensional elements library, but for the sake of our consideration special cable and membrane elements had to be constructed. The structure of the element subroutine, shown in Fig. 6, consists of eight steps used in the calculation process depending on the algorithm. This may be easily prepared for any type of element as well as difference star and should be written in C or FORTRAN language.

In order to solve a highly nonlinear boundary value problem using NAFDEM code, a special data transmission subsystem was developed. This is based on the element (node; star) information packet which consists of its main characteristics. The structure of the information packet is configured by the user in order to deliver all values required in the iteration process. Currently, the system is capable of analysing the structures modelled by one- two- and three-dimensional isoparametric elements. Moreover the coupling of the finite element and difference methods can be carried out at various stages of the numerical analysis and is still developed [14] in case of very complex engineering boundary problems in local and global formulation.

5. Numerical examples

The main idea of the finite element modelling of the behaviour of cable and membrane structures under a compressive regime is based on the iterative algorithm (see Fig. 4). At the beginning of the iteration process the structure has both tensile and compressive rigidity and after first solution the geometry is updated and the strain–stress state is calculated. Then the cable axial forces are analysed in order to eliminate compression. If the cable internal force is going to be negative this force is set to zero using the assumption of lack of cable compressive rigidity. Next, the residual forces are calculated as a difference between applied external and internal forces. The process is repeated until the convergence is achieved.

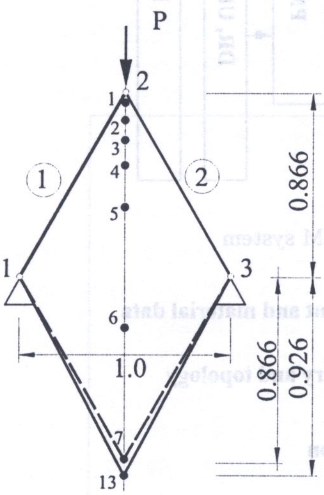

Fig. 7. Deformation of two cables system loaded at the apex

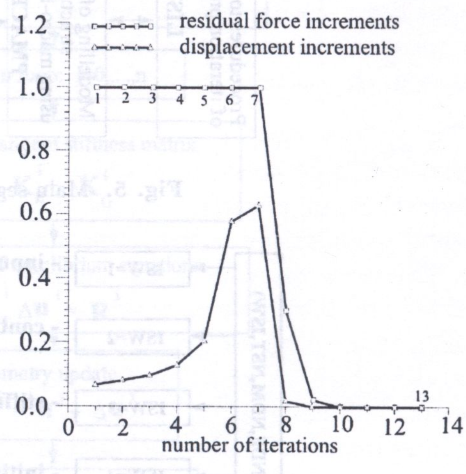

Fig. 8. Convergence of iteration process

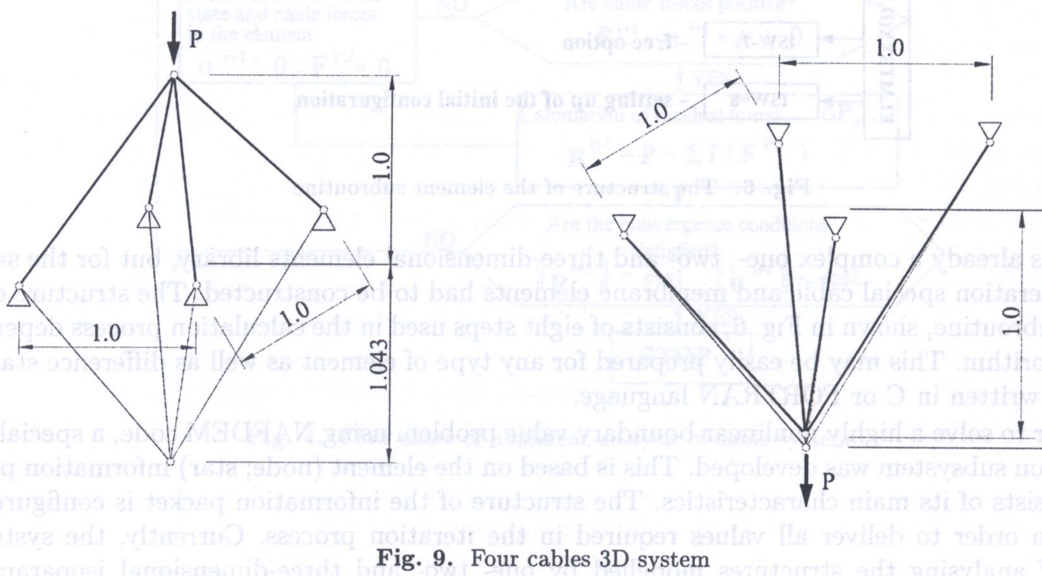

Fig. 9. Four cables 3D system

The NAFDEM computer system presented above was used to solve a number of tests. As an initial test the system of two cables with tensile rigidity of $EA = 10.0$ N was loaded by a concentrated force $P = 1.0$ N as shown in Fig. 7. The final equilibrium configuration was found after 13 iterations and positions of the loaded node 2 on the path to reach an inverted shape have been depicted in this figure, numbered 1,2,...,7. The convergence of the iteration process was depicted in Fig. 8. It may be easily seen that elements in the system are compressed through the first seven iterations and do not produce any cable reactions. Hence the residual forces remain equal to the applied load P during the iteration process. After the 7th iteration the cables start to work in tension. As a simple verification test a concave cable system was analysed (dashed lines in Fig. 7) and the same final configuration was achieved. These results were repeated in the case of the three-dimensional cable system presented in Fig. 9. Now the sudden jump of the residual forces and displacement increments caused by the singularity of the system in the stage close to the plane is observed (see Fig. 10).

Next a three-dimensional system with supports in different vertical planes was analysed. The structure is built of three cables fixed at nodesr 1 and 3 while node 2 is a roller supported in $\{yz\}$ plane. The geometry of the system was shown in Fig. 11. The material and load parameters were the same as in the previous test. After the deformation, cable 1–2 slack inwards while cable 1–3 rotated under the applied load. The only working cable was the tensile element 3–2′ shown in Fig. 11. Its

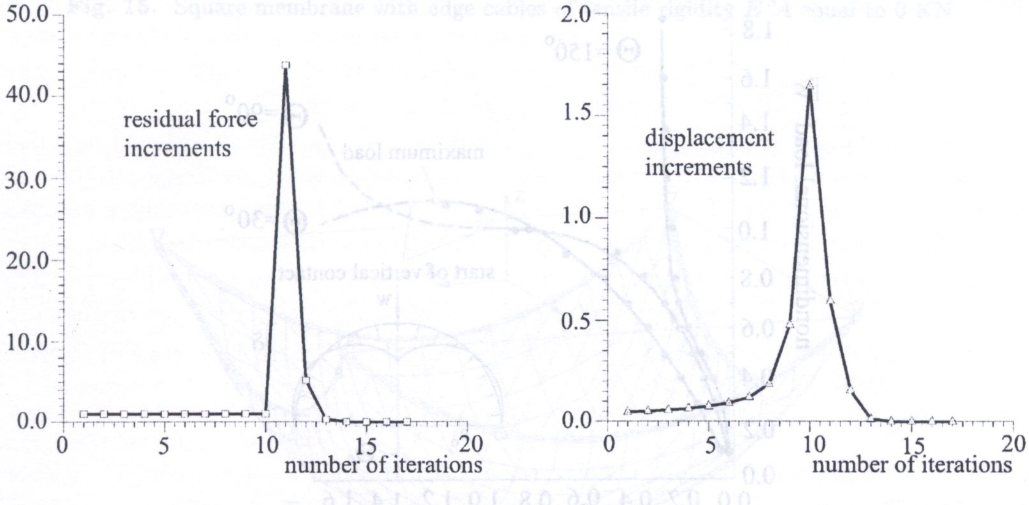

Fig. 10. Convergence of iteration process in case of four cables system

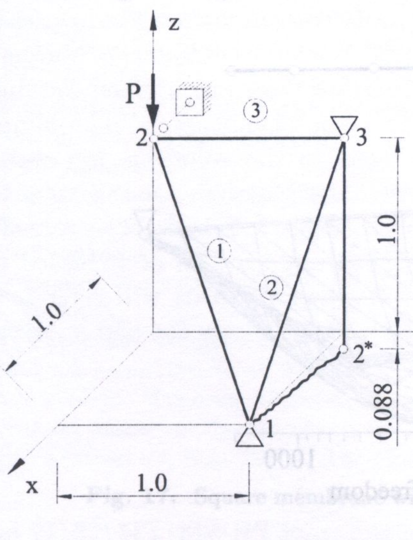

Fig. 11. Three-dimensional cable system

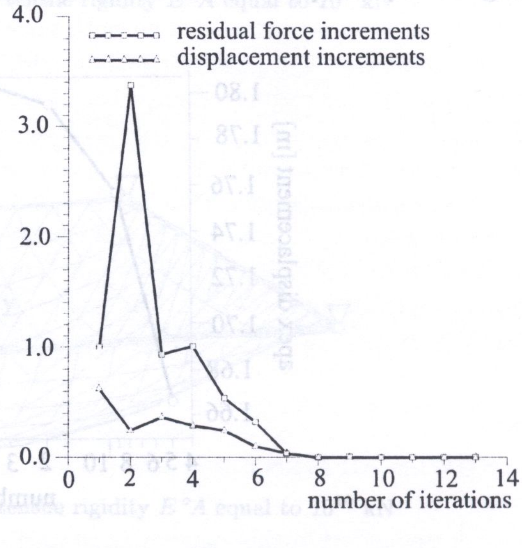

Fig. 12. Convergence of iteration process

elongation was the same as for the separate cable hung vertically at point 3 and loaded by the concentrated force P at node 2. The solution was obtained within 13 iterations and the process was depicted in Fig. 12 in terms of residual force values and displacement increments. Similarly to the previous test the first seven iterations were used to rotate the system to the stable position.

A cylindrical membrane of infinite length subject to vertical uniform apex line load was analysed next. Because of the symmetry of the load, geometry and boundary conditions this analysis can be reduced to two dimensions and only the the cross section of the membrane may be considered. The structure was depicted in Fig. 13. For the convergence test the cross section of the membrane was discretized with 3 to 1000 elements and the displacements obtained in the key versus number of degrees of freedom are depicted in Fig. 14. It may be found that about 50 elements have to be used to get the error of the solution below 0.03%. Several further solutions were obtained for different load levels and different membrane profiles, with half of the central angle $\theta_o = 30°, 90°, 150°$. Resulting load–deflection curves obtained by FEM were presented in Fig. 13 by dots in nondimensional values $\{\overline{\delta}, \overline{W}\}$ where $\overline{W} = \frac{W}{pR_o}$ and $\overline{\delta} = \frac{\delta}{R_o}$, and compared with the results obtained by the numerical integration technique in [7] (continuous lines).

Interaction of the cables and the membrane in the case of the rectangular membrane reinforced with cables along the edges (Fig. 1) was analysed next. The square with 5.0 m side length and

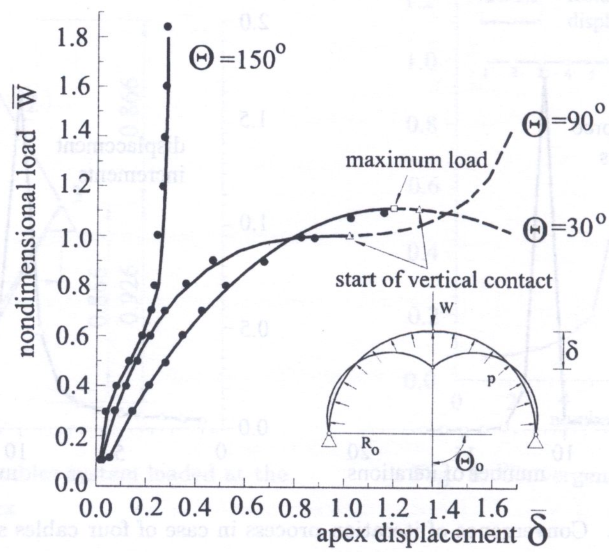

Fig. 13. Apex displacement vs. load for cylindrical membranes of infinite length calculated by FEM and NIT

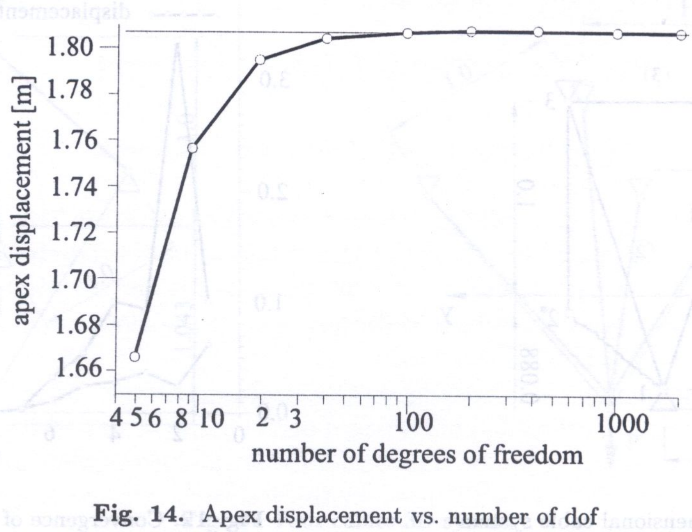

Fig. 14. Apex displacement vs. number of dof

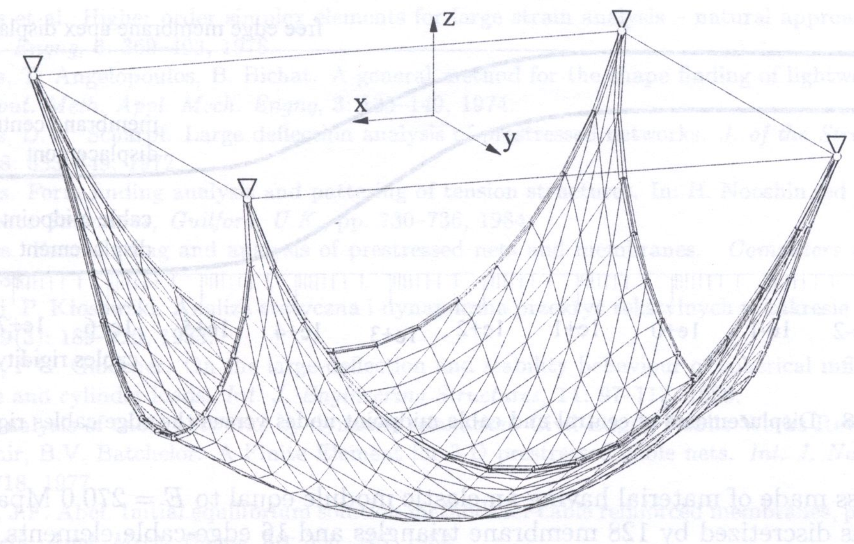

Fig. 15. Square membrane with edge cables of tensile rigidity E^oA equal to 0 KN

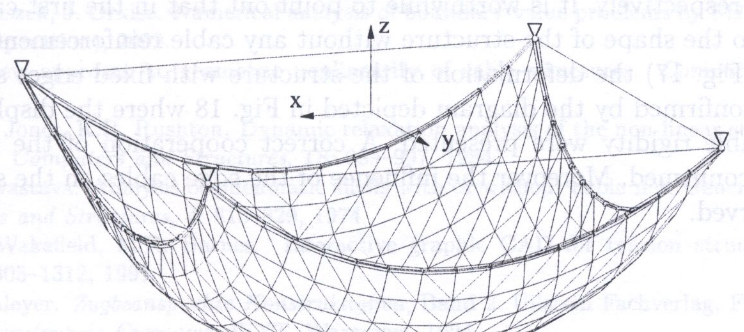

Fig. 16. Square membrane with edge cables of tensile rigidity E^oA equal to 10^3 kN

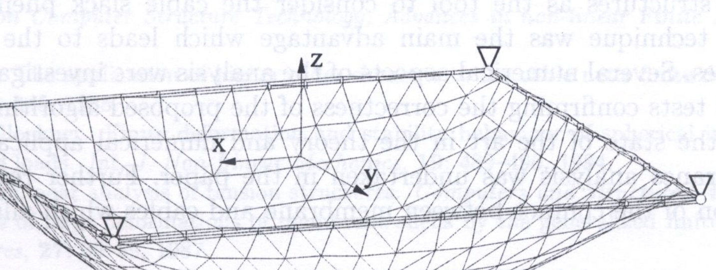

Fig. 17. Square membrane with edge cables of tensile rigidity E^oA equal to 10^{10} kN

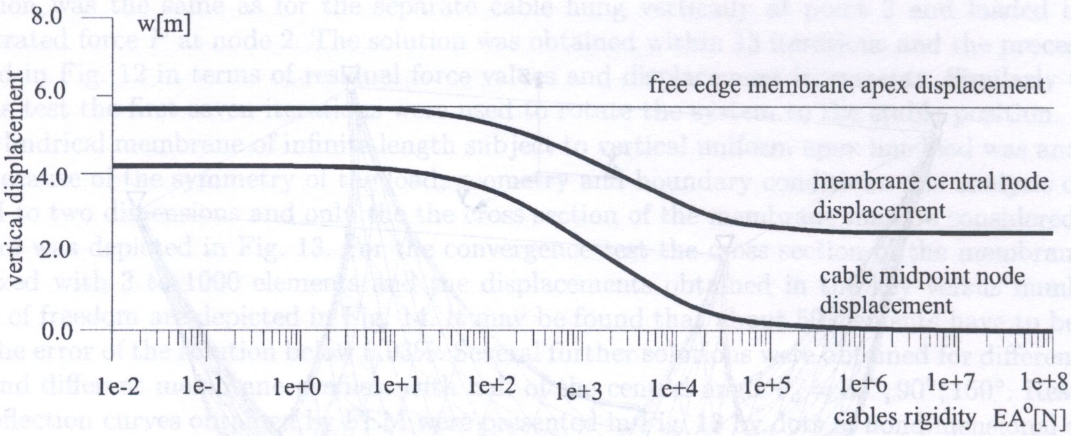

Fig. 18. Displacements of central and cable midpoint nodes versus the edge cables rigidity

0.001 m thickness made of material having an elastic module equal to $E = 270.0$ Mpa and Poisson's ratio $\nu = 0.4$ was discretized by 128 membrane triangles and 16 edge-cable elements in one quarter of the structure. In the calculation process the tension rigidity E^oA of the cables was changed from 0 kN to 10^{10} kN. The structure was loaded by a distributed pressure load of 50 kPa intensity. An initial fictitious prestress on the structure had to be introduced to start the calculations. After a couple of iterations this prestress was removed. The deformed shapes of the structure in the three cases of cable rigidity close to zero, equal to 10^3 kN, and 10^{10} kN were calculated and presented in Figs. 15, 16, and 17 respectively. It is worthwhile to point out that in the first case the deformation should correspond to the shape of the structure without any cable reinforcement whereas in case of high cable rigidity (Fig. 17) the deformation of the structure with fixed edges should be obtained. These results were confirmed by the diagram depicted in Fig. 18 where the displacements of chosen nodes versus the cable rigidity were presented. A correct cooperation of the membrane and the cable elements was confirmed. Moreover the influence of the edge cables on the size of the structure deformation is observed.

6. Conclusions

In the present paper the application of the finite element method to the analysis of large deformations of cable reinforced membrane shells with membrane wrinkling and cable slack allowed was presented. The most attention was paid to the algorithm for taking the cable slack into account, assuming their lack of compressive rigidity. Hence based on [22] the simple *cable analogy* was applied for complex cable reinforced structures as the tool to consider the cable slack phenomenon. The simplicity of the proposed technique was the main advantage which leads to the solutions for even very complex structures. Several numerical aspects of the analysis were investigated. Among other things simple numerical tests confirming the correctness of the proposed algorithm have been solved. The effort to review the state of the art in the theory and numerical applications of wrinkled cable-reinforced membranes analysis was undertaken in the paper. Further research will refer to more precise description of the contact between membrane and cables which allows the slip analysis.

Acknowledgement

The work presented in this paper was in part carried out under the grant PB-543/T11/99/17 funded by the State Committee for Scientific Research. The author gratefully acknowledges this support.

REFERENCES

[1] J.H. Argyris et al. Higher order simplex elements for large strain analysis – natural approach. *Comput. Meth. Appl. Mech. Engng*, **6**: 369–403, 1978.

[2] J.H. Argyris, T. Angelopoulos, B. Bichat. A general method for the shape finding of lightweight tension structures. *Comput. Meth. Appl. Mech. Engng*, **3**: 135–149, 1974.

[3] J.H. Argyris, D.W. Scharpf. Large deflection analysis of prestressed networks. *J. of the Struct. Division, Proc. of ASCE*, **98**: 633–649, 1972.

[4] M.R. Barnes. Form-finding analysis and pattering of tension structures. In: H. Nooshin, ed., *Proc. of IIIrd Int. Conf. on Space Structures, Guilford, U.K.*, pp. 730–736, 1984.

[5] M.R. Barnes. Form-finding and analysis of prestressed nets and membranes. *Computers and Structures*, **30**: 685–695, 1988.

[6] Cz. Branicki, P. Kłosowski. Analiza statyczna i dynamiczna przekryć tekstylnych w zakresie nieliniowym. *Arch. Inż. Ląd.*, **29**(3): 189–220, 1983.

[7] A.K. Dacko, P.G. Glockner. On the large-deflection and stability behaviour of spherical inflatables under symmetric plate and cylinder loads. *Int. J. Engineering Structures*, **11**: 97–112, 1989.

[8] A.S. Day. Analysis of cable networks by dynamic relaxation. Civil Engng Public Works Rev. **4**: 383–386, 1970.

[9] M.I. Gambhir, B.V. Batchelor. A Finite Element for 3-D prestressed cable nets. *Int. J. Numer. Meth. Engng*, **11**: 1699–1718, 1977.

[10] R.B. Haber, J.F. Abel. Initial equilibrium solution methods for cable reinforced membranes, part I – formulation. *Comput. Meth. Appl. Mech. Engng*, **30**: 335–346, 1982.

[11] R.B. Haber, J.F. Abel. Initial equilibrium solution methods for cable reinforced membranes, part II – implementation. *Comput. Meth. Appl. Mech. Engng*, **30**: 285–306, 1982.

[12] P. Kneen. Long span cable supported roof structures. Proc. of IASS – CSCE International Congress on *Innovative Large Span Structures, Concept, Design, Construction*, Toronto: 327–342, 1992.

[13] J. Krok, J. Orkisz, M. Stanuszek. A unique FDM/FEM system of discrete analysis of boundary-value problems in mechanics. Proc. of XI Polish Conf. on *Computer Methods in Mechanics*, **1**: 465–473, 1993.

[14] J. Krok, M. Stanuszek, J. Orkisz. Numerical analysis of boundary-value problems by FDM/FEM computer code NAFDEM (in preperation), 2002.

[15] A.S. Kwan. A new approach to geometric nonlinearity of cable structures. *Computers and Structures*, **67**: 243–252, 1998.

[16] W.J. Lewis, M.S. Jones, K.R. Rushton. Dynamic relaxation analysis of the non-linear static response of pretensioned cable roof. *Computers and Structures*, **18**: 989–997, 1984.

[17] C.T. Li, N.K. Srivastava. Analysis of pneumatic shells with or without cable net; General finite element formulation. *Computers and Structures*, **4**: 813–829, 1974.

[18] C.F. Ong, D.S. Wakefield, M.R. Barnes. Interactive graphic CAD for tension structures. *Computers and Structures*, **41**: 1305–1312, 1991.

[19] F. Otto, F.K. Schleyer. *Zugbeanspuchte Konstruktionen*, Band 2. Ullstein Fachverlag, Frankfurt, Berlin, 1962.

[20] Sz. Pałkowski. *Konstrukcje Cięgnowe*. WNT, Warszawa, 1994.

[21] H.J. Schek. The force density method for form finding and computations of general networks. *Comput. Meth. Appl. Mech. Engng*, **3**: 115–134, 1974.

[22] M. Stanuszek. FE analysis of large deformations of membrane shells with wrinkling. *Int. J. Finite Elements in Analysis and Design* (in print), 2002.

[23] M. Stanuszek, W. Bereza. Local stability of flexible membranes under concentrated loads – FEM analysis. *Proc. of ECCOMAS96 Conf. Paris*, **4**: 103–106, 1996.

[24] M. Stanuszek, J. Orkisz. Finite element analysis of membrane cable reinforced structures at large deformations. *Proc. of 2nd Congress on Computer Structure Technology, Advances in non-linear Finite Element Methods* **4**: 67–76, Athens, 1994.

[25] M. Stanuszek, J. Orkisz. The application of higher order elements to the cable net's finite deformation analysis. *Arch. Inż. Ląd.*, **31**: 423–445, 1985.

[26] W. Szyszkowski, P.G. Glockner. Finite deformation and stability behaviour of spherical inflatables under axisymmetric concentrated loads. *Int. J. Non-Linear Mechanics*, **19**: 489–496, 1984.

[27] B. Tabarrok, Z. Qin. Nonlinear analysis of tension structures. *Computers and Structures*, **45**: 973–984, 1992.

[28] W. Tworzydło. Analysis of large deformations of membrane shells by the generalized finite difference method. *Computers and Structures*, **27**: 39–59, 1987.

[29] D. Wakefield. Membrane engineering – principles and applications. In: T.T. Lan, ed., *Proc. of Asia-Pacific Int. Conf. on Shells and Spatial Structures, Beijing, China*, **1**: pp. 407–418, 1996.

[30] O.C. Zienkiewicz, R.L. Taylor. *The Finite Element Method*. McGraw-Hill, 1984.